Paramagnetic Anisotropy in Cobalt(II) Schiff-base Complexes. *X*-Ray Crystal Structure and Electron Spin Resonance of *NN'*-Ethylenebis(acetylacetoneiminato)cobalt(II)-doped *NN'*-Ethylenebis(acetylacetoneiminato)nickel(II)

By **Franco Cariati** * and **Franca Morazzoni**, Istituto di Chimica Generale e Inorganica, Via G. Venezian, 21 20133 Milano, Italy
Carlo Busetto, Gastone Del Piero, and **Alessandro Zazzetta**, L.S.R. Snam Progetti, San Donato Milanese, Milano, Italy

The e.s.r. study of a single crystal of *NN'*-ethylenebis(acetylacetoneiminato)cobalt(II)-doped *NN'*-ethylenebis(acetylacetoneiminato)nickel(II), [Co(acacen)] and [Ni(acacen)], is reported; determination of the ground state of the cobalt complex was attempted. [Ni(acacen)] Is isomorphous with [Co(acacen)] as shown by a single-crystal structural determination: the doped crystals are orthorhombic, space group $Pna2_1$, $Z = 4$, $a = 12.18(1)$, $b = 10.28(1)$, and $c = 10.37(1)$. The equatorial principal axes of the *g* tensor were found to be almost parallel with the cobalt–ligand bond, rather than between these bonds, as expected.

PARAMAGNETIC anisotropy measurements may be considered the best method of investigating the ground state of cobalt(II) in Schiff-base complexes, in order to provide an explanation of their oxygen-carrier properties. However, conditions for obtaining well-resolved e.s.r. spectra of these compounds have only been found in the last five years.[1–3] *NN'*-Ethylenebis(acetylacetoneiminato)cobalt(II) [Co(acacen)] gave clearly detectable e.s.r. signals in a mixed powder, [Co(acacen)] : [Ni(acacen)] 2 : 98%,[1] and the random orientation of the paramagnetic centres suggested a tentative assignment of the principal values of the magnetic tensors. An unambiguous assignment could only be derived by single-crystal analysis. A preparative method has now been found for obtaining single crystals of [Co(acacen)], [Ni(acacen)], and of [Co(acacen)]-doped [Ni(acacen)]. A detailed e.s.r. investigation on the doped sample has been carried out.

EXPERIMENTAL

[Co(acacen)] and [Ni(acacen)] were obtained by methods previously described.[4] A mixed powder of [Co(acacen)] (2%) and [Ni(acacen)] (98%) was obtained by evaporation of a chloroform solution containing the components in this ratio. Slow sublimation at 180 °C under vacuum (10^{-2} mmHg) gave dark orange needle crystals of [Co(acacen)]-doped [Ni(acacen)]. Sublimation of a powder of [Co(acacen)] or [Ni(acacen)] gave needle crystals of each of the two compounds and suggested a new method of obtaining pure samples. For the former, sublimation also prevented contamination by any oxygen impurity or by clathrated solvent molecules in the crystals.[5]

Preliminary examination of the needle-shaped crystals of [Co(acacen)]-doped [Ni(acacen)] was by Weissenberg photography. Crystals were orthorhombic, with space group $Pna2_1$ or P_{nam}. The first was assumed and subsequently confirmed by the successful refinement of the structure.

Crystal Data.—$C_{12}H_{18}N_2NiO_2$, $M = 281.0$, Orthorhombic, $a = 12.18(1)$, $b = 10.28(1)$, $c = 10.37(1)$ Å, $U = 1\,297.8$ Å^3, $F(000) = 592$. $D_c = 1.44$ g cm^{-3}, $z = 4$. Space group $Pna2_1$. Mo-K_α radiation, $\lambda = 0.710\,7$ Å; μR(Mo-K_α) = 0.5.

Final cell dimensions were determined by a least-squares fit to the setting angles measured for 23 reflections on a diffractometer. Intensity data were collected from a crystal 0.25 × 0.40 mm, mounted with the *c* axis parallel to the ϕ axis of a four-circle Siemens AED automated diffractometer, by use of Mo-K_α radiation. A total number of 1 491 independent reflections were measured (max. $\sin\theta/\lambda$ 0.64 Å^{-1}) by use of the θ—2θ scan method and the five-point technique.[6] 1 289 reflections, with intensities $I > 3\sigma(I)$, were considered observed and used in the structure determination.

The intensity of a standard reflection (400), monitored every 15 reflections, did not fluctuate by >3%. Intensities were corrected for Lorentz and polarisation effects and then scaled by Wilson's statistical method. No absorption correction was made owing to the low value of μR.

From *X*-ray analysis, single crystals of [Co(acacen)] and [Ni(acacen)] were found to be isomorphous. E.s.r. spectra were recorded only on the doped single crystal, since the undiluted [Co(acacen)] single crystal gave no signals. Measurements were made on a Varian 4 502 spectrometer at 113 K. A single crystal was mounted as described in ref. 7 and spectra were recorded at 6° intervals, by rotating the crystal around the three laboratory axes. The orientations of the laboratory axes with respect to the crystal axes had been previously determined. The *g* values were evaluated by standardisation with DPPH.

Structure Determination and Refinement.—The crystal structure was solved by Patterson and Fourier methods. Refinement was carried out by block-diagonal least-squares methods, using isotropic and anisotropic temperature factors. When *R* was reduced to 0.068, a ΔF map was computed and the 18 hydrogen atoms were located; their coordinates were then slightly adjusted to agree with the usual carbon geometry. In the last two cycles, hydrogen atoms were refined by use of isotropic thermal parameters and a damping factor of 0.4, to reduce the calculated shifts. The final value of *R* was 0.029. The function minimized

---

[1] C. Busetto, F. Cariati, P. Fantucci, D. Galizzioli, F. Morazzoni, and V. Valenti, *Gazzetta*, 1972, **102**, 1040.

[2] C. Busetto, F. Cariati, A. Fusi, M. Gullotti, F. Morazzoni, A. Pasini, and R. Ugo, *J.C.S. Dalton*, 1973, 754.

[3] C. Busetto, F. Cariati, P. Fantucci, D. Galizzioli, and F. Morazzoni, *J.C.S. Dalton*, 1973, 1712.

[4] P. J. McCarthy, R. J. Horey, K. Ueno, and A. E. Martell, *J. Amer. Chem. Soc.*, 1955, **77**, 5820.

[5] S. Bruckner, M. Calligaris, G. Nardin, and L. Randaccio, *Inorg. Chim. Acta*, 1968, **2**, 386.

[6] W. Hoppe, *Acta Cryst.*, 1969, **A25**, 67.

[7] D. B. Russell, *J. Chem. Phys.*, 1965, **43**, 1966.

TABLE 1

Atomic co-ordinates ($\times 10^4$) and anisotropic temperature factors ($\times 10^2$) for non-hydrogen atoms with estimated standard deviations in parentheses

	x/a	y/b	z/c	B_{11}	B_{22}	B_{33}	B_{12}	B_{13}	B_{23}
Ni	1 338(1)	348(1)	2 484(2)	379(2)	330(1)	346(2)	5(2)	0(3)	9(3)
O(1)	1 723(1)	1 847(3)	3 393(3)	521(14)	335(11)	462(14)	17(11)	−19(13)	−29(12)
O(2)	2 562(3)	−332(3)	3 312(3)	506(14)	387(13)	498(15)	80(11)	−142(13)	−63(12)
N(1)	105(3)	1 087(4)	1 731(4)	363(14)	459(15)	405(15)	32(13)	15(13)	91(14)
N(2)	1 004(3)	−1 173(3)	1 624(4)	430(15)	384(14)	428(16)	−51(12)	−12(14)	−56(14)
C(1)	1 776(7)	4 022(5)	4 112(7)	1 107(42)	342(19)	689(34)	42(25)	3(34)	−55(22)
C(2)	1 243(4)	2 961(5)	3 308(5)	713(28)	401(18)	420(21)	68(19)	137(20)	18(16)
C(3)	308(5)	3 208(5)	2 621(6)	765(26)	513(19)	413(26)	219(20)	116(25)	56(25)
C(4)	−240(4)	2 286(5)	1 866(4)	456(20)	603(23)	342(17)	156(18)	129(16)	152(18)
C(5)	−1 292(4)	2 718(6)	1 180(6)	509(24)	770(34)	663(33)	206(24)	9(22)	175(28)
C(6)	−530(5)	158(6)	957(8)	598(27)	554(25)	892(40)	−41(23)	−197(29)	55(28)
C(7)	108(5)	−996(6)	684(7)	623(30)	724(29)	677(32)	39(26)	−163(26)	−131(30)
C(8)	1 179(6)	−3 462(5)	893(7)	878(37)	460(22)	730(35)	−23(24)	−95(31)	−199(25)
C(9)	1 519(4)	−2 297(4)	1 713(4)	565(22)	406(18)	349(18)	−26(16)	33(17)	−53(16)
C(10)	2 418(4)	−2 476(4)	2 456(6)	660(21)	378(15)	459(20)	102(15)	−3(31)	131(27)
C(11)	2 898(4)	−1 507(4)	3 265(5)	494(20)	371(17)	415(20)	48(15)	−60(17)	−8(16)
C(12)	3 900(5)	−1 802(6)	4 063(7)	723(32)	596(28)	714(34)	220(26)	−238(28)	−59(28)

was $\Sigma w(F_o - F_c)^2$ by use of Cruickshank's weighting scheme.[8] Atomic scattering factors were taken from ref. 9.

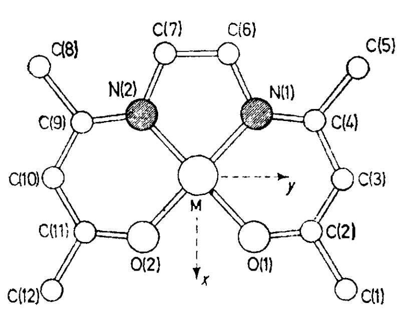

FIGURE 1 Numbering scheme for the atoms of the complex molecule (M = Co or Ni)

TABLE 2

Atomic co-ordinates ($\times 10^4$) and isotropic temperature factors ($\times 10^2$) for hydrogen atoms,* with estimated standard deviations in parentheses

	x/a	y/b	z/c	B/Å^2
H(1,1)	1 643(48)	3 735(52)	5 005(62)	482(151)
H(1,2)	1 457(56)	4 890(67)	3 734(84)	679(193)
H(1,3)	2 567(55)	4 019(65)	3 993(83)	775(202)
H(3)	−24(46)	4 146(52)	2 613(80)	612(161)
H(5,1)	−1 061(63)	3 611(66)	1 429(84)	942(220)
H(5,2)	−1 977(75)	2 348(84)	1 496(84)	1 307(270)
H(5,3)	−1 348(60)	2 681(78)	166(86)	877(231)
H(6,1)	−744(52)	466(53)	19(66)	566(159)
H(6,2)	−1 149(57)	−61(73)	1 629(88)	790(199)
H(7,1)	−407(44)	−1 650(49)	718(59)	374(119)
H(7,2)	471(51)	−802(60)	−141(63)	623(166)
H(8,1)	1 028(62)	−3 183(68)	28(76)	791(207)
H(8,2)	470(61)	−3 802(63)	1 155(76)	831(204)
H(8,3)	1 678(58)	−4 214(66)	830(83)	727(185)
H(10)	2 781(49)	−3 363(55)	2 536(94)	709(157)
H(12,1)	4 365(60)	−1 943(69)	3 625(78)	890(215)
H(12,2)	3 817(63)	−2 450(88)	4 543(108)	1 045(265)
H(12,3)	4 241(79)	−945(84)	4 509(104)	1 357(301)

* Numbered according to the carbon atom to which they are attached.

Computer programs used were written by Immirzi.[10] Final co-ordinates of the atoms are reported in Tables 1 and 2, and principal geometric parameters in Table 3. Structure factors are listed in Supplementary Publication No. SUP **21713** (7pp).* The labelling of the atoms is shown in Figure 1.

TABLE 3

Bond lengths (Å) and valence angles (°), with estimated standard deviations in parentheses

(*a*) Distances			
Ni–O(1)	1.866(3)	Ni–O(2)	1.857(3)
Ni–N(1)	1.856(4)	Ni–N(2)	1.845(4)
O(1)–C(2)	1.289(6)	O(2)–C(11)	1.276(5)
N(1)–C(4)	1.310(6)	N(1)–C(6)	1.467(8)
N(2)–C(7)	1.475(8)	N(2)–C(9)	1.317(6)
C(1)–C(2)	1.518(8)	C(2)–C(3)	1.367(8)
C(3)–C(4)	1.398(7)	C(4)–C(5)	1.532(7)
C(6)–C(7)	1.446(9)	C(8)–C(9)	1.527(8)
C(9)–C(10)	1.407(7)	C(10)–C(11)	1.375(7)
C(11)–C(12)	1.505(8)		
(*b*) Angles			
O(1)–Ni–O(2)	82.8(1)	O(1)–Ni–N(1)	94.5(1)
O(1)–Ni–N(2)	177.5(3)	O(2)–Ni–N(1)	176.9(2)
O(2)–Ni–N(2)	94.7(1)	N(1)–Ni–N(2)	88.0(1)
Ni–O(1)–C(2)	125.8(3)	Ni–O(2)–C(11)	126.6(3)
Ni–N(1)–C(4)	126.8(3)	Ni–N(1)–C(6)	113.0(3)
Ni–N(2)–C(7)	112.2(2)	Ni–N(2)–C(9)	127.1(3)
C(4)–N(1)–C(6)	120.1(2)	C(7)–N(2)–C(9)	120.4(2)
C(1)–C(2)–C(3)	120.6(3)	C(1)–C(2)–O(1)	113.9(2)
C(3)–C(2)–O(1)	125.4(2)	C(2)–C(3)–C(4)	124.3(2)
C(3)–C(4)–C(5)	117.6(2)	C(3)–C(4)–N(1)	123.0(2)
C(5)–C(4)–N(1)	119.4(2)	C(7)–C(6)–N(1)	110.9(3)
C(6)–C(7)–N(2)	111.7(2)	C(8)–C(9)–C(10)	116.7(2)
C(8)–C(9)–N(2)	121.3(2)	C(10)–C(9)–N(2)	121.9(2)
C(9)–C(10)–C(11)	124.7(2)	C(10)–C(11)–C(12)	119.8(2)
C(10)–C(11)–O(2)	124.7(2)	C(12)–C(11)–O(2)	115.5(2)

E.s.r. Results.—The spectrum observed when the magnetic field lies in a plane different from the crystal planes showed the signals of four magnetically inequivalent molecules. The e.s.r. spectra in the crystal *ab*, *ac*, and *bc* planes consisted of two sets of eight lines, one for each couple of magnetically equivalent molecules. The magnetic sets became concident when the magnetic field was parallel to a crystal axis. These results are in agreement with the crystal structure which shows a total of four molecules per unit cell, two sets of two equivalent molecules in the

---

* See Notice to Authors No. 7 in *J.C.S. Dalton*, 1975, Index issue.

[8] D. N. J. Cruickshank in, 'Computing Methods and the Phase Problem in Crystallography,' ed. J. S. Rollet, Pergamon Press, London, 1965, p. 114.

[9] F. H. Moore, *Acta Cryst.*, 1963, **16**, 1169.

[10] A. Immirzi, *Ricerca Sci.*, 1967, **37**, pp. 847, 850; *J. Appl. Cryst.*, 1973, **6**, 246.

crystal planes and four equivalent molecules along the crystal axes.

The elements of the G^2 tensors may be derived from the plots of the angular dependence of the g values, whose experimental values were obtained by averaging the results of several measurements. The accuracy of g^2 values was estimated by plotting the function (symbols have their usual meaning):

$$f(\theta) = \tfrac{1}{2}(g_{ii}^2 + g_{jj}^2) + \tfrac{1}{2}(g_{ii}^2 - g_{jj}^2)\cos 2\theta + g_{ij}^2 \sin 2\theta$$

against θ and comparing f(θ) with the experimental curve.[11] By this method the error in the determined g values was found to be ±5°. An evaluation of the experimental plots gave rise to eight different G^2 tensors, in accordance with the total ambiguity in the three crystal planes.

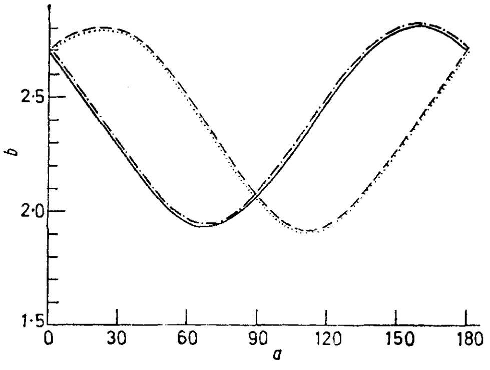

FIGURE 2 Variation of the g value as a function of rotation in the *ab* plane

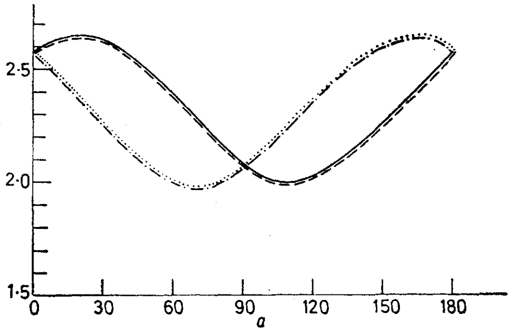

FIGURE 3 Variation of the g value as a function of rotation in the *ac* plane

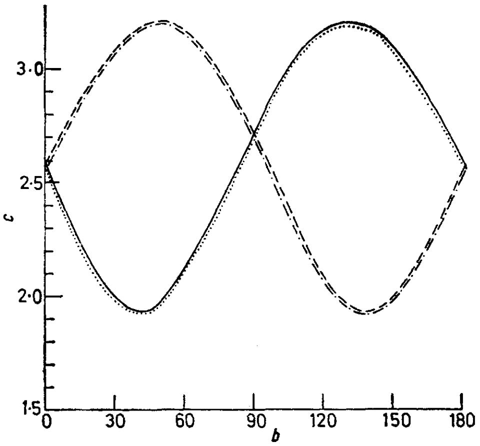

FIGURE 4 Variation of the g value as a function of rotation in the *bc* plane

The tensors may be divided into two sets of four and, within one set, the eigenvalues are the same. The four tensors whose eigenvalues are different from the principal g values obtained from the polycrystalline sample (spectrum recorded on crushed doped crystals) were eliminated. Therefore the four tensors, which differ only in the sign of g_{ij}^2 elements ($i \neq j$), corresponding to the four molecules in the unit cell, were obtained; the couplings between these four tensors and the experimental $g(\theta)$ curves are reported in Figures 2—4 where each pair of curves indicates the coincidence of the signals of different molecules in the unit cell. Particular care is now necessary in separating and correctly assigning to each molecule its tensor. Assignment of the tensors to each magnetic site in the cell was carried out as follows:

(*a*) The large-dashed and dash-dot lines of the plot of the angular dependence of the g values, in the crystal *bc* plane, gain their maximum (3.19) *ca.* 50° from the *c* axis (see Figure 4). The value almost approaches the highest of the principal g values, g_{22} (3.26); hence this direction in the *bc* plane approaches the g_{22} vector direction.

(*b*) The four inequivalent molecules in the unit cell may be divided into two sets of two molecules in the crystal planes, hence the molecule quoted in Table 3 may be associated with one set in the planes.

(*c*) The molecule quoted in Table 3 was at first tentatively assigned to the large-dashed and dash-dot lines in the *bc* plane. A schematic representation of this molecule referred to the crystal axes (Figure 5) showed that the direction having the g value 3.19, in the *bc* plane [see (*a*)], is quite close to the O(1)–Co–N(2) bond direction. It can therefore be concluded that, in this assignment, the g_{22} direction is very close to the O(1)–Co–N(2) direction.

(*d*) The assignment of the molecule quoted in Table 3 to the large-dashed or dash-dot line should give a relatively large g value in the *ba* plane, at *ca.* 20° from the *b* axis, which is the angle between the *b* axis and the projection of the direction O(1)–Co–N(2) in this plane.

(*e*) It is seen that the conclusion in (*d*) is more correct for the large-dashed line (g 2.8) than for the dash-dot line (g 2.4) (at *ca.* 20° from the *b* axis, see Figure 2). Therefore the molecule quoted in Table 3 may be reasonably assigned to the large-dashed line. In this case g_{11} and g_{22} are the principal in-plane and g_{33} the principal out-of-plane g values [Figure 5(a)]; the g_{22} direction is very close to the direction of the O(1)–Co–N(2) bond, that of g_{11} to the direction of the O(2)–Co–N(1) bond, and g_{33} is almost coincident with the *z* molecular axis.

(*f*) The molecule quoted in Table 3 may alternatively be assigned to the full line or small-dashed line. In this case, in the *bc* plane, at *ca.* 40° from the *x* axis, the minimum value (g 1.93) is gained (Figure 4). The value approaches g_{11} 1.88 or g_{33} 2.00 and the direction of g_{11} or g_{33} could be considered nearly coincident with the direction of the O(1)–Co–N(2) bond.

(*g*) From considerations similar to those in (*b*)—(*d*), the assignment of the full and small-dashed lines, in the *ba* plane, to the molecule quoted in Table 3, should give $g \simeq$ 2.00 at *ca.* 20° from the *b* axis. This conclusion was not found to accord well with experimental data for the full (g 2.44) or for the dashed line (g 2.88) (see Figure 2). However, even on assigning the molecule to the full line (the assignment to the small-dashed line is extremely improbable), g_{11} and g_{22} were still obtained as the in-plane g values [see Figure 5(d)], and with the directions exchanged with respect to the assignment to the large-dashed line.

The molecule quoted in Table 3 is best assigned to the large-dashed line; an assignment to the solid line could lead only to an exchange of the in-plane g values. Assignment to the large-dashed line is the only one which shows g_{11}, g_{22}, and g_{33} directions remaining almost the same with respect to the molecular axes, in the three crystal planes (Figure 6).

All the foregoing arguments may be considered qualitative proof of the correct coupling between each G^2 tensor and the

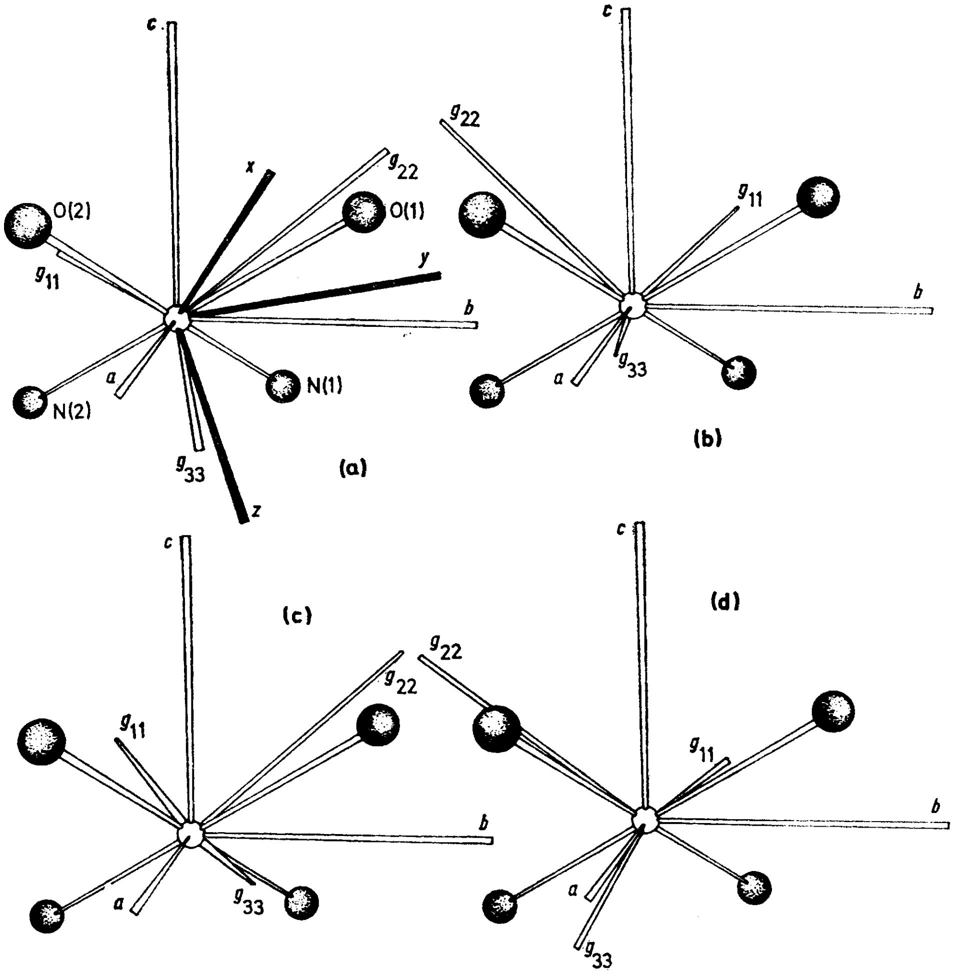

FIGURE 5 Schematic representation of the molecule quoted in Table 3 and of the principal magnetic axes with respect to the crystal axes. The principal magnetic axes correspond to (a) the large-dashed, (b) the small-dashed, (c) the dash-dot and (d) the full line

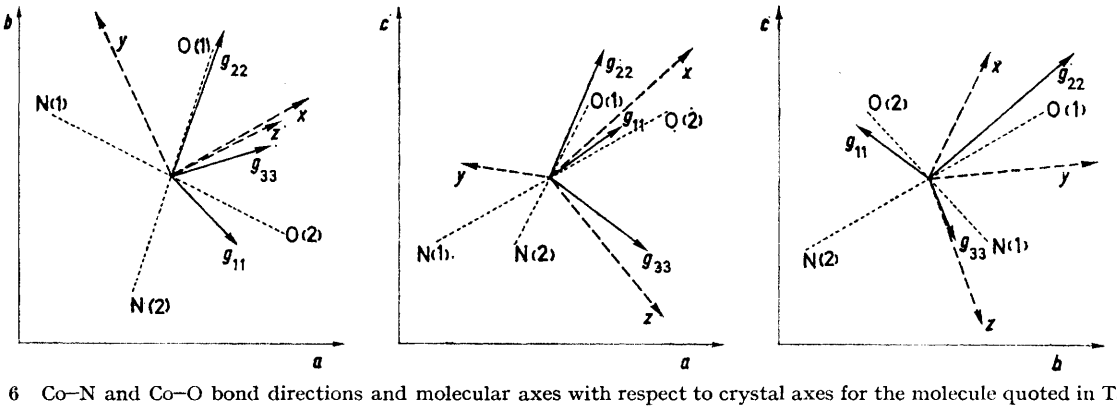

FIGURE 6 Co–N and Co–O bond directions and molecular axes with respect to crystal axes for the molecule quoted in Table 3. Orientations of the principal g values interpolated form the large dashed line in Figures 2—4 with respect to crystal axes

corresponding molecule; however in the case of [Co(acacen)], numerical resolution of the assignment proved impossible.

The conclusions of our analysis are in accord with results of an e.s.r. investigation on samples in the nematic phase,[12] data from which may be reasonably accepted as an integral part of the single-crystal analysis.

The principal g values, their orientations with respect to the crystal axes, and the angles between the crystal and molecular axes (Table 4), show the definitive orientations of the magnetic with respect to the molecular axes. The analogous anisotropic analysis of the hyperfine interactions proved impossible, because the extensive overlapping of the splitting, due to inequivalent molecules, led to a poor evaluation of the hyperfine components.

DISCUSSION

The g value assignments derived from the data of Table 4 are as follows: g_{11} and g_{22} to g values in the molecular plane, and g_{33} to the out-of-plane value.

TABLE 4

Angles (°) with respect to the crystal axes

g values		c	b	a
g_{11}	1.8807	61° 6′	129° 36′	53° 6′
g_{22}	3.2639	50° 48′	43° 12′	74° 42′
g_{33}	2.0074	127° 18′	75° 18′	40° 54′
Molecular axes *				
Y		86° 18′	24° 24′	114° 6′
X		49° 48′	72° 24′	45° 24′
Z		139° 30′	73° 24′	54° 18′
Bond directions *				
O(2)–Co–N(1)		65° 54′	115° 30′	38° 13′
O(1)–Co–N(2)		59° 52′	31° 3′	78° 2′

* Data are referred to the molecule in Figure 1.

This assignment differs from that suggested for the powder spectra[1] by the reverse assignment of g_{11} and g_{33}. However it agrees with that obtained from the nematic phase spectra.[12] In our assignment, the principal out-of-plane g value is intermediate between the in-plane values, and this order is surprisingly different from that of many other cobalt low-spin compounds with analogous molecular symmetry. The most usual order shows the g in-plane values to be both larger than the out-of-plane g value.[13,14]

As regards the position of the magnetic with respect to the molecular axes, no one of the magnetic axes was found to be coincident with the C_2 axis, taken as usual for a C_{2v} symmetry; the equatorial magnetic axes lie in the molecular plane almost parallel to the N–Co–O bonds and only the out-of-plane magnetic axis has been found to be nearly coincident with the molecular z axis.

These results, though surprising, are not impossible to understand, because the four molecules of [Co(acacen)] lie in four different sites of C_1 symmetry. Hence there is no reason for a magnetic principal direction, related to the crystal-symmetry properties, to be coincident with the C_2 axis, which is related to the molecular symmetry properties. The values of A, which were obtained for powdered samples, have been assumed as principal values and associated with respect to their g values. The large displacement of the g_{22} value from the free-electron value showed that the ground-state determination could not be treated by a first-order approximation. Hence, the expressions of the g and A principal values have been calculated by a second-order approximation,[2] assuming as the X magnetic axis, the axis N(2)–Co–O(1), and as Y axis, the axis O(2)–Co–N(1). The Z axis obviously lies perpendicular to the molecular plane.

Two ground-state configurations, $(xz)^2(xy)^2(yz)(z^2)^2$ and $(xz)^2(xy)^2(yz)^2(z^2)$, could be in agreement with the experimental magnetic values; and in both cases the difference between these two configurations was not $>2\,000$ cm^{-1}. The experimental and the calculated g and A values, together with the P values and the Fermi constant values, are reported in Table 5. The d orbital mixing coefficients b_i and c_i, for both possible ground-states have also been reported. The expressions for the g and A magnetic parameters, which are different from those reported in ref. 2, owing to change of the magnetic axes, are reported in Table 6. It is worth noting that, while the g_{xx} value and the A values agree very satisfactorily with those found experimentally, the experimental g_{yy} and g_{zz} values are not readily reproducible. Whatever is the ground state configuration, the calculated value of g_{zz} is found to be too small and that of g_{yy} too large. In addition the energy-level trend, derived from the mixing coefficients c_i, when the unpaired electron is in the d_{yz} orbital, and the trend derived from b_i coefficients, when the unpaired electron is the d_{z^2} orbital, both agree with the experimentally observed d–d transitions to the same extent.[1] For these reasons it is not possible to unambiguously assign the ground-state configuration and a large mixing between $(xz)^2(xy)^2(yz)(z^2)^2$ and $(xz)^2(xy)^2(yz)^2(z^2)$ has to be considered. Nevertheless, our model for the calculation confirmed that the unpaired electron lies mainly out of the molecular plane, and is available to be

TABLE 6

g and A expressions for the ground-state $(xz)^2(xy)^2(yz)(z^2)^2$, calculated by a second-order approximation, with the three-hole formalism

$$g_{zz} = 2c_5^2 + 2c_2^2 - 2c_3^2 - 2c_1^2 - 2c_4^2 - 4c_2c_5$$

$$g_{xx} = 2c_5^2 - 2c_2^2 - 2c_3^2 + 2c_1^2 + 2c_4^2 - 4\sqrt{3}\ c_1c_5 - 4c_2c_3 + 4c_4c_5$$

$$g_{yy} = 2c_5^2 - 2c_2^2 + 2c_3^2 - 2c_1^2 - 2c_4^2 - 4c_3c_5 + 4\sqrt{3}\ c_1c_2$$

$$\begin{aligned} A_{zz} = 2P[&1/7c_5^2 - 2c_2c_5 + 3/7c_3c_5 - \sqrt{3}/7c_1c_5 - 3/7c_4c_5 \\ &+ 1/7c_2^2 - 3/7c_2c_3 - \sqrt{3}/7c_1c_2 + 2/7c_3^2 - 2/7c_1^2 \\ &+ 2/7\ c_4^2 - k/2(c_5^2 + c_2^2 - c_3^2 - c_1^2 - c_4^2)] \end{aligned}$$

$$\begin{aligned} A_{xx} = 2P[&-2/7c_5^2 - 1/7c_3^2 - 1/7c_1^2 + 1/7c_4^2 - 1/7c_2^2 - 3/7c_2c_5 \\ &- 3/7c_3c_5 - 2\sqrt{3}\ c_1c_5 + 2c_4c_5 - 2c_2c_3 - \sqrt{3}/7c_1c_2 \\ &- 2\sqrt{3}/7c_1c_3 - k/2(c_5^2 - c_2^2 - c_3^2 + c_1^2 + c_4^2)] \end{aligned}$$

$$\begin{aligned} A_{yy} = 2P[&1/7c_5^2 + 2/7c_2^2 + 1/7c_3^2 + 1/7c_1^2 - 1/7c_4^2 + 3/7c_2c_5 \\ &- 2c_3c_5 + \sqrt{3}/7c_1c_5 + 3/7c_4c_5 - 3/7c_2c_3 + 2\sqrt{3}c_1c_2 \\ &- 2\sqrt{3}/7c_1c_3 - k/2(c_5^2 - c_2^2 + c_3^2 - c_1^2 - c_4^2)] \end{aligned}$$

Expression for c_i from ref. 2.

---

[11] J. R. Morton, *Chem. Rev.*, 1964, **64**, 453.

[12] B. M. Hoffman, F. Basolo, D. L. Diemente, *J. Amer. Chem. Soc.*, 1973, **95**, 6497.

[13] A. H. Maki, N. Edelstein, A. Devison, and R. H. Holm, *J. Amer. Chem. Soc.*, 1964, **86**, 4580.

[14] R. B. Bentley, F. E. Mabbs, N. R. Smail, M. Gerloch, and J. Lewis, *J. Chem. Soc.* (*A*), 1970, 3003.

TABLE 5

Experimental g and A values, with calculated values in parentheses [a]

Ground-state configuration							
	g_{zz}	g_{xx}	g_{yy}	A_{zz} [b]	A_{xx} [b]	A_{yy} [b]	
	2.00	3.26	1.88	34.5	115.8	37.5	
	(1.87)	(3.24)	(2.05)	(34.5)	(115.8)	(37.5)	
	c_1	c_2	c_3	c_4	c_5	P [b]	k
$(xz)^2(xy)^2(yz)(z^2)^2$	−0.2064	−0.0359	−0.0664	−0.0035	0.9556	186	0.26
	$E_{yz} - E_{z^2}$ [c]	$E_{yz} - E_{xz}$	$E_{yz} - E_{xy}$	$E_{yz} - E_{x^2-y^2}$			
	(*ca.* 1700)	8 000	5 000	(57.000)			
		(*ca.* 6 000)	(3 000)				
	g_{zz}	g_{xx}	g_{yy}	A_{zz} [b]	A_{xx} [b]	A_{yy} [b]	
	2.00	3.26	1.88	34.5	115.8	37.5	
	(1.89)	(3.21)	(2.12)	(34.5)	(115.8)	(−37.5)	
	b_1	b_2	b_3	P [b]	k		
$(xz)^2(xy)^2(yz)^2(z^2)$	−0.1803	−0.0380	0.9829	175	0.28		
	$E_{z^2} - E_{yz}$	$E_{z^2} - E_{xz}$					
	(1900)	8 000					
		(*ca.* 9 000)					

[a] Expressions for c_i and b_i from ref. 2. [b] $cm^{-1} \times 10^4$. [c] Spin–orbit coupling constant has been assumed to be 400 cm^{-1}.

transferred to molecular oxygen. The energy-level trends suggested here suggest that, even if the ground state has the configuration $(xz)^2(xy)^2(yz)(z^2)^2$, a feeble axial perturbation, deriving from a base molecule, may be sufficient to obtain the electronic configuration $(xz)^2(xy)^2(yz)^2(z^2)$, which is considered the most favourable to the reaction with oxygen.[3]

Our results are not completely in agreement with those reported by Zelewsky [15] for *NN'*-ethylenebis(salicylideneiminato)cobalt(II), [Co(salen)], although a mixing between the two low-lying energy states has also been found in this compound. Recently, Basolo *et al.*[11] have suggested a ground-state configuration $(xz)^2(xy)^2(yz)^2(z^2)$, with the premise that the magnetic axes bisect the O(2)–Co–O(1) and the O(1)–Co–N(1) angles. With this choice of axes now ruled out by the single-crystal analysis, the ground-state $(xz)^2(xy)^2(yz)(z^2)^2$ is impossible to obtain, because the mixing coefficients were not all negative.[2,3]

We thank the Italian C.N.R. for financial support of this research.

[4/1646 *Received, 5th August,* 1974]

---

[15] A. V. Zelewsky and H. Fiers, *Helv. Chim. Acta.*, 1973, **56**, 977.